

One-Dimensionally Extended Paddlewheel Dirhodium Complexes from Metal–Metal Bonds with Diplatinum Complexes

Kazuhiro Uemura* and Masahiro Ebihara*

Department of Chemistry, Faculty of Engineering, Gifu University, Yanagido 1-1, Gifu, 501-1193, Japan

Supporting Information

ABSTRACT: We have succeeded in obtaining unique one-dimensional (1D) chain complexes (**1**, **2**, and **3**) comprised of two types of metal species: rhodium and platinum. These compounds are constructed from a dinuclear rhodium complex (i.e., $[\text{Rh}_2]$) and a pivalamidate-bridged platinum complex (i.e., $[\text{Pt}_2]$), forming an attractive quasi-1D infinite chain, expressed as $-\{[\text{Rh}_2]-[\text{Pt}_2]-[\text{Pt}_2]\}_n-$. Interestingly, the bridging ligands of $[\text{Rh}_2]$ can be varied with trifluoroacetate, acetate, and acetamidate groups, indicating the possibility of electronic structure modulation in the 1D chain.

Paddlewheel dinuclear complexes have a rich redox chemistry and show various electronic configurations based on the metal–metal bond orbitals.¹ They are useful modules for assembled structures because the axial sites are available for coordination of linker ligands.^{2–6} Direct interactions between the metal–metal bonds, or those across a ligand, are interesting from the viewpoint of materials science, and recent efforts have been reported on the construction of dimensional arrangements of paddlewheel-type dinuclear complexes.^{1–6} For example, dinuclear ruthenium complexes linked by TCNQ (7,7,8,8-tetracyanoquinodimethane) derivatives produce characteristic donor–acceptor systems with ligand-controlled charge transfer,^{2b} and I^- -bridged $[\text{Rh}_2(\text{acam})_4]^{0/+}$ (acam = acetamidate), having a mixed oxidation state three-dimensional (3D) diamondoid network, shows characteristic electrical conductivity.^{3b} Although there exists a large number of unique assembled structures with various linker ligands, such as organic molecules,² halide ions,³ π -conjugated molecules,⁴ coordination compounds,⁵ and inorganic molecules,⁶ to the best of our knowledge, $[\{\text{Rh}_2(\text{O}_2\text{CCF}_3)_2(\text{CO})_4\}_2]_n$ ⁷ is the only compound so far where different metal ions bridge paddlewheel dinuclear complexes.

The compound $[\{\text{Rh}_2(\text{O}_2\text{CCF}_3)_4\}\{\text{Rh}_2(\text{O}_2\text{CCF}_3)_2(\text{CO})_4\}_2]_n$ was obtained by accident in the sublimation of $[\text{Rh}_2(\text{O}_2\text{CCF}_3)_4]$.⁷ The overall structure is an extended linear chain with a repeat unit of $-\{[\text{Rh}_2^{\text{II,II}}]-[\text{Rh}_2^{\text{I,I}}]-[\text{Rh}_2^{\text{I,I}}]\}_n-$, where each dinuclear complex is linked with direct metal–metal bonds. In this 1D chain complex, interactions between the vacant σ^* orbitals of $[\text{Rh}_2^{\text{II,II}}]$ and the filled σ^* of $[\text{Rh}_2^{\text{I,I}}]$ effectively support the formation of the metal–metal bonds along the chain. Taking advantage of such interaction, we have tried to rationally construct a 1D chain complex to make a contribution to this field.⁸ Here, we show a new type of 1D chain complex comprised of paddlewheel dirhodium complexes and platinum complexes with direct metal–metal interactions (Scheme 1).

We selected $[\text{Pt}_2(\text{piam})_2(\text{NH}_3)_4]^{2+}$ (where *piam* = pivalamidate) instead of $[\text{Rh}_2(\text{O}_2\text{CCF}_3)_2(\text{CO})_4]$ for the module of our 1D chain complexes, because both compounds have the same electronic configuration of $\sigma^2\pi^4\delta^2\delta^*\pi^*4\sigma^*2$. Simply mixing $[\text{Rh}_2(\text{O}_2\text{CCF}_3)_4]$ and $[\text{Pt}_2(\text{piam})_2(\text{NH}_3)_4](\text{CF}_3\text{CO}_2)_2$ in a ratio of 1:2 in EtOH, followed by slow evaporation, afforded single crystals of $[\{\text{Rh}_2(\text{O}_2\text{CCF}_3)_4\}\{\text{Pt}_2(\text{piam})_2(\text{NH}_3)_4\}_2]_n(\text{CF}_3\text{CO}_2)_{4n}\cdot 2n\text{EtOH}\cdot 2n\text{H}_2\text{O}$ (**1**), having a metallic luster. Figure 1a shows the crystal structure of **1**.⁹ The most remarkable structural feature is the paddlewheel dinuclear complexes of $[\text{Rh}_2(\text{O}_2\text{CCF}_3)_4]$ sandwiched by $[\text{Pt}_2(\text{piam})_2(\text{NH}_3)_4]^{2+}$ at both ends with metal–metal bonds to form $[\text{Pt}_2]-[\text{Rh}_2]-[\text{Pt}_2]$ units, where a crystallographic inversion center lies at the center of the rhodium complex. The platinum dinuclear complexes are bonded to a rhodium complex with a bond distance of $\text{Pt}(2)-\text{Rh}(1) = 2.7473(15)$ Å and a typical torsion angle $\text{N}-\text{Pt}-\text{Rh}-\text{O}$ of about 45° . Multiple hydrogen bonds between the nitrogen atoms of the amine/amidate ligands in the platinum complexes and the carboxylate oxygen atoms in the rhodium complex with an $\text{N}-\text{O}$ bond distance of 3.00–3.26 Å support these unbridged metal–metal bonds. The hexanuclear $[\text{Pt}_2]-[\text{Rh}_2]-[\text{Pt}_2]$ segments are linked by quadruple hydrogen bonds between the oxygen atoms of the *piam* groups and the nitrogen atoms of the ammine ligands, resulting in the formation of a quasi-1D infinite chain, expressed as $-\{[\text{Rh}_2]-[\text{Pt}_2]-[\text{Pt}_2]\}_n-$, where the linked platinum dinuclear complexes form the tetranuclear platinum backbone $[\text{Pt}_2]-[\text{Pt}_2]$, similar to “platinum blue” compounds.¹⁰

Interestingly, this type of 1D chain complex can be diversely designed. When $[\text{Rh}_2(\text{O}_2\text{CCH}_3)_4]$ or $[\text{Rh}_2(\text{acam})_4]$ units are selected as the dinuclear rhodium parts, each mixture with $[\text{Pt}_2(\text{piam})_2(\text{NH}_3)_4]^{2+}$ affords single crystals, $[\{\text{Rh}_2(\text{O}_2\text{CCH}_3)_4\}\{\text{Pt}_2(\text{piam})_2(\text{NH}_3)_4\}_2]_n(\text{PF}_6)_{4n}\cdot 6n\text{H}_2\text{O}$ (**2**) and $[\{\text{Rh}_2(\text{acam})_4\}\{\text{Pt}_2(\text{piam})_2(\text{NH}_3)_4\}_2]_n(\text{CF}_3\text{CO}_2)_{4n}$ (**3**),¹¹ respectively. As shown in Figure 1b and c, both **2** and **3** show 1D chain complexes similar to **1**, expressed as $-\{[\text{Rh}_2]-[\text{Pt}_2]-[\text{Pt}_2]\}_n-$. Compound **2** crystallizes in the triclinic space group $P\bar{1}$ with cell parameters to similar **1**. Despite the weaker Lewis acid of $[\text{Rh}_2(\text{O}_2\text{CCH}_3)_4]$ versus $[\text{Rh}_2(\text{O}_2\text{CCF}_3)_4]$,¹ a similar 1D chain complex is attained. Compared with both **1** and **2**, the 1D chains in **3** undulate, because the $[\text{Pt}_2]$ and $[\text{Pt}_2]$ groups in **3** are not stacked face-to-face but in a twisted fashion (Figure 1c, right; Table S2, Supporting Information) that is associated with the formation of hydrogen bonds between the $[\text{Pt}_2]$ and CF_3CO_2^- groups. In **3**, the $[\text{Rh}_2(\text{acam})_4]$ unit has a lower number of hydrogen bond acceptor sites compared with the tetra-carboxylate

Received: April 18, 2011

Published: July 26, 2011

complexes, where both attraction and repulsion forces coexist between the $[\text{Rh}_2]$ and $[\text{Pt}_2]$ units. Nevertheless, the $[\text{Rh}_2(\text{acam})_4]$ group affords a similar 1D chain complex, which also supports the notion that the orbital interaction of the metal–metal bonds between $[\text{Rh}_2]$ and $[\text{Pt}_2]$ is relatively strong.

Taking into account that the sum of the metal oxidation numbers of $[\text{Rh}_2]-[\text{Pt}_2]-[\text{Pt}_2]$ in **1–3** is +12, which was obtained from single-crystal X-ray analysis, each oxidation state can be considered as being $-\{[\text{Rh}_2^{\text{II,II}}]-[\text{Pt}_2^{\text{II,II}}]-[\text{Pt}_2^{\text{II,II}}]\}_n^-$, which is unchanged from that in the starting compounds. Table 1 summarizes the metal–metal bond distances of **1**, **2**, and **3** and in other reported compounds. The Rh–Rh bond distance of the paddlewheel rhodium parts (2.408(2) Å) in **1** is similar to that found in the axially water-coordinated complex $[\text{Rh}_2^{\text{II,II}}(\text{O}_2\text{C}-\text{CF}_3)_4(\text{H}_2\text{O})_2]$ (2.394(3) Å).¹² The Pt–Pt bond distance reflects the oxidation state of the platinum atoms.¹⁰ In **1**, both the Pt–Pt bond distance of the intra- (Pt(1)–Pt(2) = 2.8947(12) Å) and the inter- (Pt(1'')–Pt(1) = 3.0791(15) Å) unit distances are shorter than those of $[\text{Pt}_4^{\text{II,II,II,II}}(\text{piam})_4(\text{NH}_3)_8](\text{PF}_6)_4 \cdot 2\text{H}_2\text{O}$

(intradimer = 2.9546(11) Å, interdimer = 3.1256(12) Å) and longer than those of $[\text{Pt}_4^{\text{II,II,II,II}}(\text{piam})_4(\text{NH}_3)_8](\text{PF}_6)_4(\text{ClO}_4) \cdot 2\text{H}_2\text{O}$ (intradimer = 2.8039(9) Å, interdimer = 2.8603(12) Å).^{8e} In both **2** and **3**, a similar tendency was found in the bond distances (Table 1). X-ray photoelectron spectra (XPS) of **1** and **2** reveal that the Pt 4f_{7/2} binding energies are 73.1 and 73.4 eV (Figure S5, Supporting Information), respectively, which are closer to that of $[\text{Pt}_2^{\text{II,II}}(\text{en})_2(\alpha\text{-pyridonato})_2](\text{NO}_3)_2$ (73.1 eV; en = ethylenediamine) than to that of $[\text{Pt}_2^{\text{III,III}}(\text{NH}_3)_4(\alpha\text{-pyrrolidonato})_2(\text{NO}_3)_2](\text{NO}_3)_2$ (74.6 eV).¹³ Furthermore, the Rh 3d_{5/2} binding energies obtained were 308.9 (**1**) and 308.8 (**2**) eV, which are close to the value of $[\text{Rh}_2^{\text{II,II}}(\text{O}_2\text{CCH}_3)_4]$ (309.0 eV).¹⁴ These results also support the oxidation states of $-\{[\text{Rh}_2^{\text{II,II}}]-[\text{Pt}_2^{\text{II,II}}]-[\text{Pt}_2^{\text{II,II}}]\}_n^-$.

Although **1–3** all have the same oxidation states of $-\{[\text{Rh}_2^{\text{II,II}}]-[\text{Pt}_2^{\text{II,II}}]-[\text{Pt}_2^{\text{II,II}}]\}_n^-$, several differences were observed in their electronic spectra (Figure S6, Supporting Information) and the metal–metal bond distances. Diffuse reflectance spectra of **1** show new two bands around 464 and 670 nm instead of that at 591 nm in $[\text{Rh}_2(\text{O}_2\text{CCF}_3)_4]$, which is attributed to $\pi^* \rightarrow \sigma^*$ transition in the Rh₂ core. Similarly, in **2**, there were two new bands around 412 and 697 nm, which are not observed in $[\text{Rh}_2(\text{O}_2\text{CCH}_3)_4]$. These observations support the σ -type interaction between $[\text{Rh}_2]$ and $[\text{Pt}_2]$ and the different properties among **1–3**. Furthermore, single crystal X-ray analyses revealed that the Rh–Rh bond distance in **1** is longer than that in **2** (Table 1), which is attributed to the strong electron-withdrawing properties of the trifluoroacetate group, and the Rh–Rh bond distance in **3** is considerably longer than that of the carboxylate groups in the 1D chain complex. When the rhodium dinuclear complexes are integrated into the 1D chain complexes, the difference in the features among the parent rhodium parts may be reflected in the differences in electronic structure.

DFT calculations (Figure S7, Supporting Information) on the part of the chain, $\{[\text{Pt}_2]-[\text{Rh}_2]-[\text{Pt}_2]\}_n^{4+}$, based on the crystal

Scheme 1. 1D Chain Complexes (**1**, **2**, and **3**) Comprised of Rhodium and Platinum

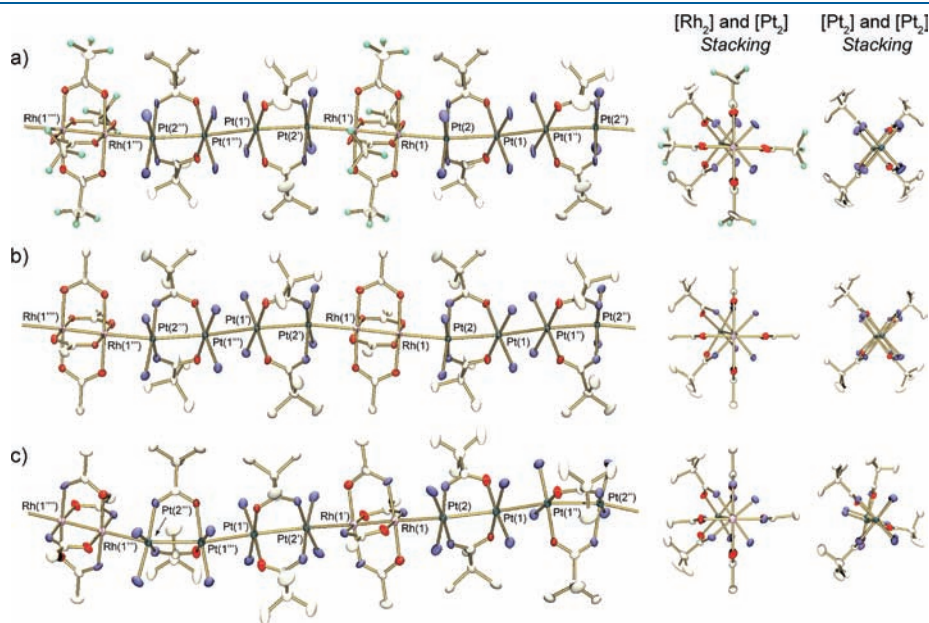
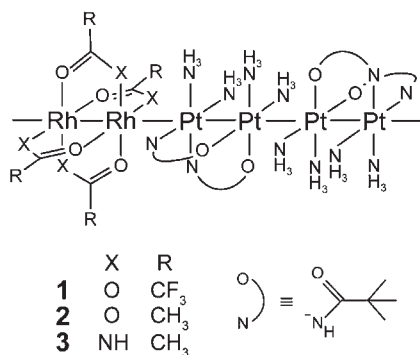


Figure 1. Crystal structures of (a) $[\{\text{Rh}_2(\text{O}_2\text{CCF}_3)_4\}\{\text{Pt}_2(\text{piam})_2(\text{NH}_3)_4\}]_n(\text{CF}_3\text{CO}_2)_{4n} \cdot 2n\text{EtOH} \cdot 2n\text{H}_2\text{O}$ (**1**), (b) $[\{\text{Rh}_2(\text{O}_2\text{CCH}_3)_4\}\{\text{Pt}_2(\text{piam})_2(\text{NH}_3)_4\}]_n(\text{PF}_6)_{4n} \cdot 6n\text{H}_2\text{O}$ (**2**), and (c) $[\{\text{Rh}_2(\text{acam})_4\}\{\text{Pt}_2(\text{piam})_2(\text{NH}_3)_4\}]_n(\text{CF}_3\text{CO}_2)_{4n}$ (**3**). The hydrogen atoms, anions, and solvent molecules are omitted for clarity. The middle and right views are stacking fashions between $[\text{Rh}_2]$ and $[\text{Pt}_2]$ or $[\text{Pt}_2]$ and $[\text{Pt}_2]$, respectively.

Table 1. Comparison of Selected Bond Distances (Å) between 1, 2, 3, and Reported Compounds.^{8c}

compounds	Rh–Rh	intra Pt–Pt	inter Pt–Pt
1	2.408(2)	2.8947(12)	3.0791(15)
2	2.3832(17)	2.9376(7)	3.0893(9)
3	2.423(2)	2.9299(9)	3.0651(12)
[Pt ₄ ^{II,II,II,II} (piam) ₄ (NH ₃) ₈] ⁴⁺		2.9546(11)	3.1256(12)
[Pt ₄ ^{II,II,II,II} (piam) ₄ (NH ₃) ₈] ⁵⁺		2.8039(9)	2.8603(12)

structures of 1–3 also indicate the difference in frontier orbitals found in 1–3. In the case of the models for both 1 and 2 having tetracarboxylate dirhodium parts, the HOMOs and LUMOs are made up from interactions between σ -type orbitals, whereas, in 3, the HOMO is the δ^* orbital of the Rh₂(acam)₄ group, which is from the π interaction with the amidate ligands, inducing a destabilization of the δ^* orbital (Figure S8, Supporting Information).¹⁵ Taking into account that the 1D chain backbones with metal–metal bonds are mainly constructed by the z -character orbitals (σ or π), it may be possible to remove the δ^* electrons of the Rh₂(acam)₄ part in 3. Because compounds constructed with interactions between metal–metal bonds are interesting, especially when they have open-shell electronic structures,^{3b,8e,8g} attempts to prepare a 1D chain complex incorporating [Rh₂(acam)₄]⁺ groups are currently in progress. In summary, our results demonstrate that linear chain structures consisting of two types of metal are formed by taking advantage of the interaction among their σ^* orbitals. Although several problems related to the yield remain, it is possible to modify bridging ligands in $-\{[\text{Rh}_2]-[\text{Pt}_2]-[\text{Pt}_2]\}_n-$ type chains toward the modulation of the electronic structure, paving the way for a synthetic methodology for such heterometallic 1D chain complexes.

■ ASSOCIATED CONTENT

S Supporting Information. Synthetic procedures, detailed crystal structures, IR spectra, XPS, diffuse reflectance spectra, DFT calculations, and crystal Information files (CIF) included. This material is available free of charge via the Internet at <http://pubs.acs.org>.

■ AUTHOR INFORMATION

Corresponding Author

*E-mail: k_uemura@gifu-u.ac.jp, ebihara@gifu-u.ac.jp.

■ ACKNOWLEDGMENT

This work was supported by Saijiro Endo Memorial Foundation for Science and Technology, Ogawa Science and Technology Foundation. Theoretical calculations were performed using the Research Center for Computational Science, Okazaki, Japan.

■ REFERENCES

- (1) Cotton, F. A.; Murillo, C. A.; Walton, R. A. *Multiple Bonds Between Metal Atoms*, 3rd ed.; Springer Science and Business Media, Inc.: New York, 2005.
- (2) (a) Handa, M.; Mikuriya, M.; Sato, Y.; Kotera, T.; Nukada, R.; Yoshioka, D.; Kasuga, K. *Bull. Chem. Soc. Jpn.* **1996**, *69*, 3483–3488. (b) Miyasaka, H.; Campos-Fernández, C. S.; Clérac, R.; Dunbar, K. R. *Angew. Chem., Int. Ed.* **2000**, *39*, 3831–3835. (c) Takamizawa, S.; Nakata,

E.-i.; Yokoyama, H.; Mochizuki, K.; Mori, W. *Angew. Chem., Int. Ed.* **2003**, *42*, 4331–4334.

(3) (a) Kitagawa, H.; Onodera, N.; Sonoyama, T.; Yamamoto, M.; Fukawa, T.; Mitani, T.; Seto, M.; Maeda, Y. *J. Am. Chem. Soc.* **1999**, *121*, 10068–10080. (b) Fuma, Y.; Ebihara, M.; Kutsumizu, S.; Kawamura, T. *J. Am. Chem. Soc.* **2004**, *126*, 12238–12239.

(4) (a) Handa, M.; Takata, A.; Nakao, T.; Kasuga, K.; Mikuriya, M.; Kotera, T. *Chem. Lett.* **1992**, 2085–2088. (b) Cotton, F. A.; Dikarev, E. V.; Petrukhina, M. A. *J. Am. Chem. Soc.* **2001**, *123*, 11655–11663. (c) Petrukhina, M. A.; Andreini, K. W.; Mack, J.; Scott, L. T. *Angew. Chem., Int. Ed.* **2003**, *42*, 3375–3379.

(5) (a) Lu, J.; Harrison, W. T. A.; Jacobson, A. J. *Chem. Commun.* **1996**, 399–400. (b) Fuma, Y.; Ebihara, M. *Chem. Lett.* **2006**, *35*, 1298–1299.

(6) Cotton, F. A.; Dikarev, E. V.; Petrukhina, M. A. *Angew. Chem., Int. Ed.* **2000**, *39*, 2362–2364.

(7) Cotton, F. A.; Dikarev, E. V.; Petrukhina, M. A. *J. Organomet. Chem.* **2000**, *596*, 130–135.

(8) (a) Finnis, G. M.; Canadell, E.; Campana, C.; Dunbar, K. R. *Angew. Chem., Int. Ed.* **1996**, *35*, 2772–2774. (b) Pruchnik, F. P.; Jakimowicz, P.; Ciunik, Z.; Stanislawek, K.; Oro, L. A.; Tejel, C.; Ciriano, M. A. *Inorg. Chem. Commun.* **2001**, *4*, 19–22. (c) Sakai, K.; Ishigami, E.; Konno, Y.; Kajiwara, T.; Ito, T. *J. Am. Chem. Soc.* **2002**, *124*, 12088–12089. (d) Mitsumi, M.; Goto, H.; Umebayashi, S.; Ozawa, Y.; Kobayashi, M.; Yokoyama, T.; Tanaka, H.; Kuroda, S.-i.; Toriumi, K. *Angew. Chem., Int. Ed.* **2005**, *44*, 4164–4168. (e) Uemura, K.; Fukui, K.; Nishikawa, H.; Arai, S.; Matsumoto, K.; Oshio, H. *Angew. Chem., Int. Ed.* **2005**, *44*, 5459–5464. (f) Hayoun, R.; Zhong, D. K.; Rheingold, A. L.; Doerrer, L. H. *Inorg. Chem.* **2006**, *45*, 6120–6122. (g) Uemura, K.; Fukui, K.; Yamasaki, K.; Matsumoto, K.; Ebihara, M. *Inorg. Chem.* **2010**, *49*, 7323–7330. (h) Doerrer, L. H. *Dalton Trans.* **2010**, *39*, 3543–3553.

(9) Yadokari-XG, Software for Crystal Structure Analyses, Wakita K. 2001; Release of Software (Yadokari-XG 2009) for Crystal Structure Analyses, Kabuto, C.; Akine, S.; Nemoto, T.; Kwon, E. *J. Cryst. Soc. Jpn.* **2009**, *51*, 218–224.

(10) (a) Barton, J. K.; Rabinowitz, H. N.; Szalda, D. J.; Lippard, S. J. *J. Am. Chem. Soc.* **1977**, *99*, 2827–2829. (b) Barton, J. K.; Szalda, D. J.; Rabinowitz, H. N.; Waszczak, J. V.; Lippard, S. J. *J. Am. Chem. Soc.* **1979**, *101*, 1434–1441.

(11) The yield of 3 was <1%. Although we were unable to obtain an elemental analysis for 3, it was possible to estimate four CF₃CO₂[−] ions per $-\{[\text{Rh}_2]-[\text{Pt}_2]-[\text{Pt}_2]\}_n-$ unit from single X-ray analysis. Detailed information is shown in the Supporting Information.

(12) Cotton, F. A.; Kim, Y. *Eur. J. Solid State Inorg. Chem.* **1994**, *31*, 525–534.

(13) Matsumoto, K.; Sakai, K.; Nishio, K.; Tokisue, Y.; Ito, R.; Nishide, T.; Shichi, Y. *J. Am. Chem. Soc.* **1992**, *114*, 8110–8118.

(14) Nefedov, V. I.; Salyn, Y. V.; Labutin, V. Y.; Baranovskii, I. B. *Koord. Khim.* **1987**, *13*, 103–105.

(15) Kawamura, T.; Katayama, H.; Nishikawa, H.; Yamabe, T. *J. Am. Chem. Soc.* **1989**, *111*, 8156–8160.